C h a p t e r 2

Mechanism of a Luminescent Dicopper System That Facilitates Electrophotochemical Coupling of Benzyl Chlorides via a Strongly Reducing Excited State

Adapted from:

Zott, M. D.; Canestraight, V. M.; Peters, J. C.

ACS Catal. **2022**, *12*, 10781–10786.

DOI: 10.1021/acscatal.2c03215.

2.1 Introduction

Photochemistry, often in conjunction with transition-metal catalysis, is growing in prominence in modern synthetic methodology.[1,2,3,4] Photochemical activation of widely available electrophiles can afford versatile reactive intermediates, such as organic radicals,[5,6] which can be leveraged in a variety of transformations.[7,8,9,10] For instance, a recent focus of a number of labs, including our own, has been to partner photochemically generated radical intermediates (R•) with copper(II)-bound N-nucleophiles in catalytic, photoinduced N-alkylations (Scheme 2.1, eqns 1 and 2; $–N_{nuc}$ denotes an amide nucleophile).[9,11,12,13,14,15,16,17,18]

Production of R• from alkyl halides is integral to many modern organic transformations,[19,20,21] and hence there is considerable interest in expanding the types of alkyl halides compatible with R• generation under synthetically useful conditions.[22,23,24] Alkyl chlorides, with potentials below −2 V vs SCE, are desirable electrophiles but are challenging to reduce;[22,25] the limited examples of their outer-sphere photochemical activation typically feature harsh conditions.[26,27,28] Phosphine-supported copper-amide excited states[29,30,31,32,33] can be more reducing than those of typical ruthenium or iridium systems,[34] providing sufficient driving force for alkyl chloride reduction. To promote photoinduced R• generation via a copper species in a generalized fashion (e.g., avoiding the subsequent C–N coupling step as in Scheme 2.1, eqn 2), the copper byproduct of oxidative quenching must be recycled by a suitable reductant.

In 1987, Sauvage demonstrated an elegant solution to photocatalyst regeneration via the electrophotochemical reduction of 4-nitrobenzyl bromide with $[Cu(dap)_2]^+$ (E_{ox}^* ~

−1.4 V; τ_0 = 0.27 μs; dap = 2,9-dianisyl-1,10-phenanthroline).[35] Organic photosensitizers have more recently been used to reduce (pseudo)halides under extremely reducing electrophotoredox conditions ($E_{ox}^* < -3$ V).[36,37,38,39] The suggested lifetimes ($\tau_0 \sim 1$ ns) and nature of the photoreductant intermediates of these processes are still under investigation.[40]

In this study, we explore a dicopper diamond core system (hereafter [Cu_2]), previously developed by our lab[33] and featuring a combination of terminal phosphine and bridging amide ligands, as an attractive electrophotoredox catalyst (Scheme 2.1, bottom).

Scheme 2.1. Electrophotochemical Organohalide Reduction.

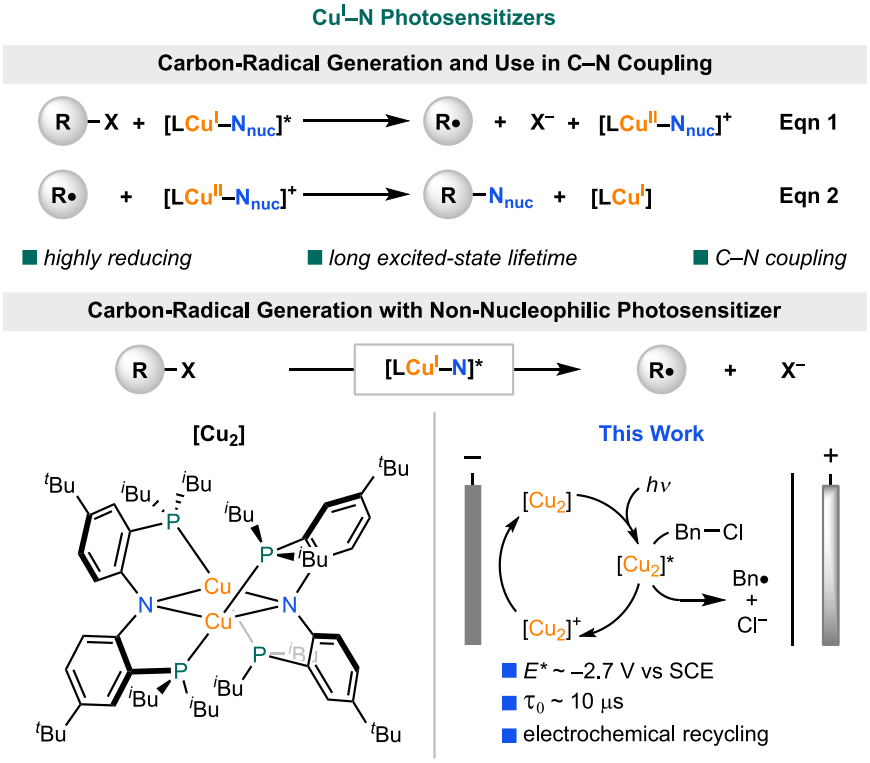

[Cu_2] is an especially strong excited-state reductant ($E_{ox}^* \sim -2.7$ V), with a long-lived excited state in solution at RT ($\tau_0 \sim 10$ μs). Charge delocalization by the $Cu_2(\mu\text{-}N)_2$ diamond core, as well as steric protection from ligand *iso*-butyl and *tert*-butyl groups, is expected to render the one-electron oxidized state $[Cu_2]^+$ non-nucleophilic. Furthermore, $[Cu_2]^+$ can be

electrochemically interconverted with $[Cu_2]$; $[Cu_2]^+$ has been isolated and characterized in the solid state.[41]

As a representative study of the excited state intermolecular photochemistry of Cu^I–amide systems, with an eye towards photoreductions using alkyl chlorides as R• precursors, we explore herein photochemically-driven, electrochemically-cycled, radical couplings using $[Cu_2]$ and benzyl chloride substates (E_p up to −2.5 V vs SCE). The dicopper system described here is mechanistically well-defined, and as we show, it is the $[Cu_2]^*$ excited state that serves as the outer-sphere photoreductant of benzyl chloride substrates; the ground-state oxidized byproduct, $[Cu_2]^+$, is electrochemically recycled to afford a catalytic, electrophotochemical C–C coupling process.

2.2 Results and Discussion

We began by investigating the reactivity of 4-methylbenzyl chloride (**1**) (E_p = −2.5 V vs SCE) as a model substrate. Benzyl chlorides are important substrates in modern synthesis and methodology[42,43,44] and also provide a convenient radical termination pathway via diffusion-limited dimerization, simplifying our mechanistic studies.[45] Exposing **1** to blue light irradiation (440 nm) in 1,2-dimethoxyethane (DME), no reaction is observed. However, when $[Cu_2]$ is added, bibenzyl product **1-D** is formed quantitatively (Figure 2.1A).

Benzyl chloride photoreduction was mechanistically interrogated via Stern-Volmer (SV) studies to establish outer-sphere electron transfer (ET) and to probe rates of ET. Time-resolved photoluminescence spectroscopy confirmed that electronically distinct benzyl chlorides **1**–**8** quench [Cu_2] in a dynamic (i.e., diffusional) process. The rates of quenching,

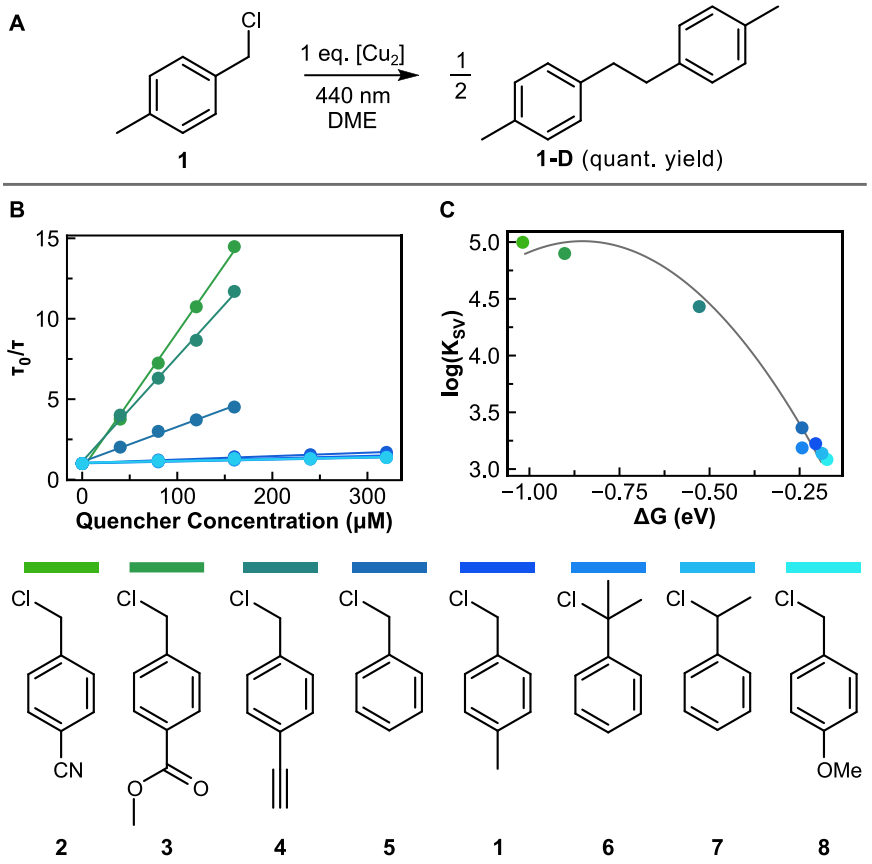

Figure 2.1. Photoreduction of benzyl chlorides. (A) Performed for 2 h with yield analyzed by ^{1}H NMR versus CH_2Br_2 internal standard. (B) Stern-Volmer quenching and (C) Marcus theory analysis in the presence of various benzyl chloride quenchers.

determined from linear SV plots (Figure 2.1B), were in the range of ~10^8 – 10^{10} $M^{-1} \cdot s^{-1}$ for K_{SV}/τ_0. These values indicate rapid quenching, reaching diffusion-limited values with electron poor **2**. Using benzyl chloride peak potentials obtained from cyclic voltammetry (E_p = −1.7 – −2.5 V; see SI), the quenching rates could be analyzed as a function of driving force, using E_{ox}^* ~ −2.7 V. Notably, a quadratic relationship between log(K_{SV}) and driving

force was observed, consistent with the behavior predicted by Marcus theory for outer-sphere electron transfer (Figure 2.1C).[46] Although such outer-sphere dynamic quenching is commonly assumed in photoredox mechanisms, this contrasts with the behavior of some organic electrophotoredox catalysts hypothesized to involve preassembly of the photocatalyst and substrate to compensate for short lifetimes.[38] These photophysical measurements thus indicate a rapid dynamic oxidative quenching step in which [Cu_2] undergoes outer-sphere electron transfer to benzyl chloride electrophiles.

We expected oxidative quenching to produce the stable, red-brown, mono-oxidized species $[Cu_2]^+$ (Figure 2.2A).[41] 440 nm irradiation of [Cu_2] and **1** in DME produces a pale-yellow solution, the UV-vis spectrum of which is mostly featureless (Figure 2.2B). Thus, the expected UV-vis features for $[Cu_2]^+$ at 520, 600, and 800 nm were not observed. Surprisingly, this suggests that the oxidative quenching reaction may involve either degradation following quenching or chemical steps at copper.

We hypothesized that the stability of $[Cu_2]^+$ could be compromised by chloride, a byproduct of benzyl chloride reductive C–Cl bond cleavage. Accordingly, addition of lithium chloride to a solution of $[Cu_2]^+$ in DME resulted in a loss of red-brown color over several hours, producing a yellow solution. Off-white crystals isolated from the reaction mixture were characterized by two ^{31}P NMR peaks (Figure 2.2C), and single-crystal XRD revealed the presence of two independent dimers, each comprised of two CuCl (chloro-cubane) or one CuCl (chloro-diamond) per H-PNP^{t}Bu ligand equivalent, i.e., [(H-PNP^{t}Bu)Cu_2(μ-Cl)$_2$]$_2$ or [(H-PNP^{t}Bu)Cu(μ-Cl)]$_2$, respectively. Independent synthesis of chloro-cubane and chloro-diamond (SI), produced white solids whose ^{31}P NMR resonances

reproduced those of the co-crystalline material (Figure 2.2C), and the characterization of chloro-diamond enabled its identification as a reaction product in the stoichiometric reaction described in Figure 2.1A (SI).

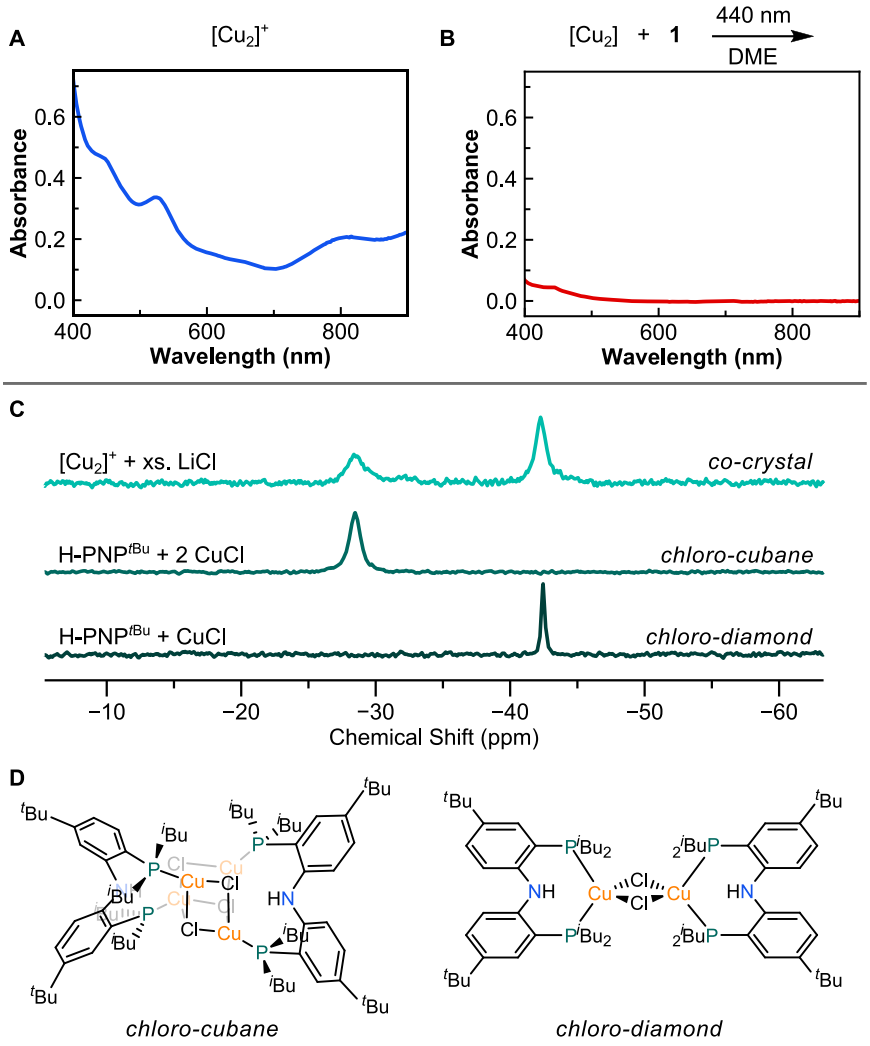

Figure 2.2. Influence of chloride on oxidized copper products. UV-vis spectra in DME of: (A) $[Cu_2]^+$ and (B) a mixture of $[Cu_2]$ and 4-methylbenzyl chloride irradiated (440 nm) for 5 minutes. (C) ^{31}P NMR spectra of chloride-bound copper products and (D) their structures.

We sought to detect and track the fate of $[Cu_2]^+$ in the presence of chloride via a UV-vis time course analysis, photolyzing $[Cu_2]$ and **1** under 440 nm irradiation (Figure 2.3A). Bands characteristic of $[Cu_2]^+$ grow in throughout 15–30 seconds, after which the 520 nm absorbance rapidly decreases. This accounts for our failure to observe the presence of $[Cu_2]^+$ in Figure 2.2B. Knowing that chloride in the form of lithium chloride slowly degrades $[Cu_2]^+$ over a period of several hours, we investigated whether lithium salts could sequester chloride via tight ion-pairing to mitigate degradation of $[Cu_2]^+$.[47]

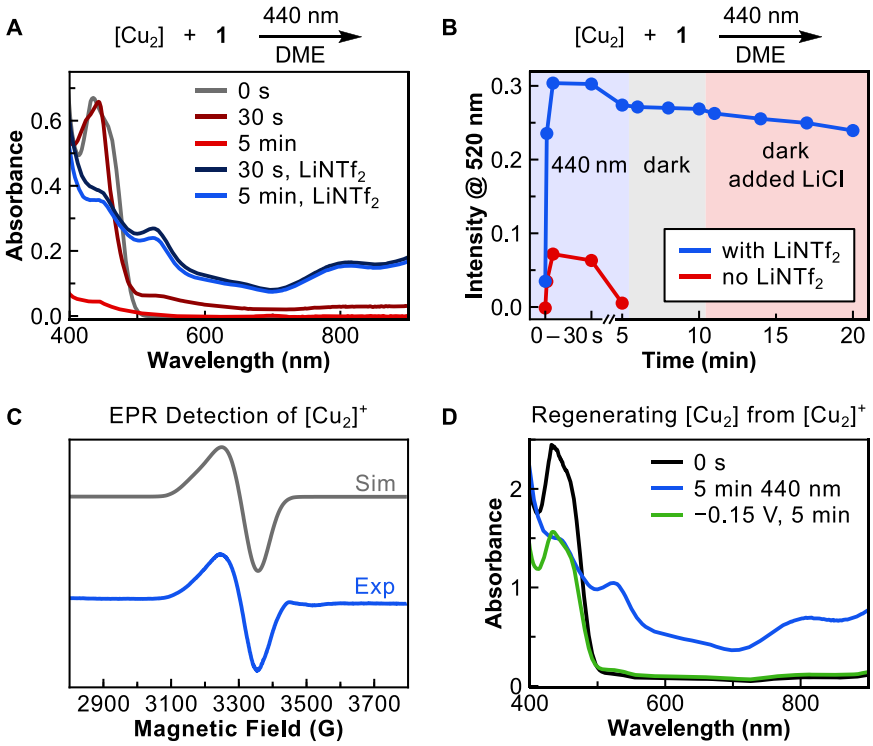

Figure 2.3. Stability and regeneration of $[Cu_2]^+$. Time course studies for a mixture of $[Cu_2]$ and **1** under 440 nm irradiation. (A) UV-vis spectra and (B) 520 nm absorbance vs time in the presence and absence of 0.2 M $LiNTf_2$. (C) 77 K EPR spectrum recorded after 15 s of irradiation in the presence of $LiNTf_2$. (D) UV-vis spectra pre- and post-irradiation, as well as following 5 minutes of −0.15 V applied potential in the dark.

When $[Cu_2]$ and **1** were irradiated in the presence of 0.2 M $LiNTf_2$, bands for $[Cu_2]^+$ became persistent, decreasing in intensity by only ~20% after 20 minutes (Figure 2.3B). This is consistent with kinetic measurements which indicate a rate of $\sim 3 \times 10^{-2}\ M^{-1} \cdot s^{-1}$

for the reaction between $[Cu_2]^+$ and tetrabutylammonium chloride in the presence of 0.2 M $LiNTf_2$; without $LiNTf_2$, the reaction is almost instantaneous (SI). Analysis of $[Cu_2]$ photolyzed in the presence of **1** and 0.2 M $LiNTf_2$ by EPR provided orthogonal support for assigning the product as $[Cu_2]^+$ (Figure 2.3C).[48] Thus, these analyses indicate $[Cu_2]^+$ to be the oxidative quenching product and corroborate its degradation by chloride.

Stabilizing $[Cu_2]^+$ enables the prospect of electrochemically regenerating $[Cu_2]$. $[Cu_2]^+$ was photochemically generated from $[Cu_2]$ and **1** in DME, with $LiNTf_2$ serving as both a chloride sequestrant and the electrolyte, then transferred into a two-compartment electrochemical cell. Applying $E_{app} = -0.15$ V for 5 minutes using a carbon cloth working electrode, cathodic of $E_{ox} = 0$ V for $[Cu_2]^{0/+}$, 0.76 e^- equivalents of current were passed (Figure 2.3D). One electron is required to fully reduce $[Cu_2]^+$ to its photoactive neutral state, thus up to 76% could be reduced. The UV-vis spectrum of this solution showed recovery of the 440 nm peak characteristic for $[Cu_2]$, albeit with ~60% of its original intensity, indicating successful, albeit incomplete, regeneration.[49] Electrochemical analysis of chloro-cubane and chloro-diamond indicated no electron transfer pathway for recovering $[Cu_2]$ at our operating potential, highlighting the importance of stabilizing $[Cu_2]^+$ and rationalizing the incomplete regeneration of $[Cu_2]$.

The described reactivity of the $[Cu_2]$ system constitutes the requirements for an electrophotoredox cycle (Scheme 2.1), so we turned to catalytic investigations under controlled potential conditions (Table 2.1). Indeed, $[Cu_2]$ is a competent electrophotoredox catalyst, generating **1-D** from **1** in 89% yield using 3 mol % $[Cu_2]$ (entry 1). Additional substrates **2**–**8** proceeded in 68–91% yield (entries 12–18). No reaction was observed in

the absence of either [Cu_2] or light (entries 2–3). In the absence of an applied potential, only the expected stoichiometric amount of **1-D** relative to [Cu_2] was produced (entry 4).

The intermediacy of benzyl radicals during catalysis is supported by several pieces of circumstantial evidence. Production of **1-D** in the presence of added water (entry 5), as

Table 2.1. Electrophotocatalytic Benzyl Chloride Reduction.[a]

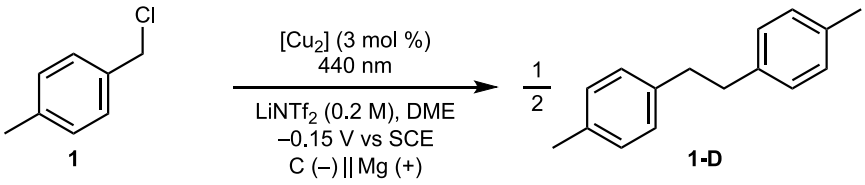

Entry	Variation	Yield[b]
1	none	90[c]
2	no [Cu_2]	0
3	no light	0
4	no applied potential	2
5	2 equiv. H_2O	62
6	5 mL air	4 {7}[d]
7	$LiClO_4$ instead of $LiNTf_2$	30
8	$TBAPF_6$ instead of $LiNTf_2$	10
9	$TBANTf_2$ instead of $LiNTf_2$	11
10	chloro-cubane instead of [Cu_2]	0
11	chloro-diamond instead of [Cu_2]	0
12	**2 → 2-D**	77[c]
13	**3 → 3-D**	77[c]
14	**4 → 4-D**	68[c]
15	**5 → 5-D**	81[c]
16	**6 → 6-D**	77[c]
17	**7 → 7-D**	91[c]
18	**8 → 8-D**	75[c]

[a]Performed for 1.5–3 h with 0.15 mmol benzyl chloride.
[b]Yields of known products determined by 1H NMR versus CH_2Br_2 internal standard.
[c]Average of two runs.
[d]Value for 4-methylbenzaldehyde in {braces}.

well as dimerization of tertiary and ester-substituted benzyl chlorides, are inconsistent with the intermediacy of benzyl anions. Although the reaction is highly sensitive to air due to quenching of $[Cu_2]^*$ (entry 6), 4-methylbenzaldehyde becomes the major product (7% yield). Benzaldehydes are known products of the reaction between benzyl radicals and oxygen.[35,50] Attempts to trap benzyl radicals with the radical trap TEMPO were unsuccessful as TEMPO quenches $[Cu_2]$.[51]

The catalytic reaction is very sensitive to factors that alter chloride binding to $[Cu_2]^+$. Li^+ from $LiNTf_2$ likely interacts with chloride through ion pairing as a Lewis acid; electrolytes expected to exhibit weaker ion pairing with chloride, such as tetrabutylammonium salts, performed notably worse (entries 7–9). The poorer performance of $LiClO_4$ (entry 7) is attributed to the fact that in DME ClO_4^- is more tightly associated to Li^+ than is NTf_2^-,[52] possibly limiting sequestration of Cl^-. Isolated chloro-cubane and chloro-diamond (Figure 2.2D) were catalytically inactive under the conditions (entries 10–11). Therefore, the detection of chloro-diamond by ^{31}P NMR at the end of the standard reaction (entry 1) suggests one pathway by which catalysis ceases.

2.3 Conclusion

To close, we have described the electrophotochemical reactivity of $[Cu_2]$ in the presence of benzyl chloride substrates. Our mechanistic studies enable assignment of facile electron-transfer from the excited state $[Cu_2]^*$ with substrate to liberate $[Cu_2]^+$, Cl^-, and a benzyl radical that undergoes homocoupling to produce bibenzyl. By tracking down off-path copper-cubane and -diamond chloride sinks, and devising a means of sequestering the chloride produced, we are able to demonstrate the electrophotocatalytic chemistry of

interest. Our study complements other recent reports employing organo-photocatalysts for R(Ar)–X electrophotochemical couplings where the nature of the photoreductants are still being studied.

2.4 References

[1] Skubi, K. L.; Blum, T. R.; Yoon, T. P. Dual Catalysis Strategies in Photochemical Synthesis. *Chem. Rev.* **2016**, *116*, 10035–10074.

[2] Genzink, M. J.; Kidd, J. B.; Swords, W. B.; Yoon, T. P. Chiral Photocatalyst Structures in Asymmetric Photochemical Synthesis. *Chem. Rev.* **2022**, *122*, 1654–1716.

[3] Chan, A. Y.; Perry, I. B.; Bissonnette, N. B.; Buksh, B. F.; Edwards, G. A.; Frye, L. I.; Garry, O. L.; Lavagnino, M. N.; Li, B. X.; Liang, Y.; Mao, E.; Millet, A.; Oakley, J. V.; Reed, N. L.; Sakai, H. A.; Seath, C. P.; MacMillan, D. W. C. Metallaphotoredox: The Merger of Photoredox and Transition Metal Catalysis. *Chem. Rev.* **2022**, *122*, 1485–1542.

[4] Romero, N. A.; Nicewicz, D. A. Organic Photoredox Catalysis. *Chem. Rev.* **2016**, *116*, 10075–10166.

[5] Studer, A.; Curran, D. P. Catalysis of Radical Reactions: A Radical Chemistry Perspective. *Angew. Chem. Int. Ed.* **2016**, *55*, 58–102.

[6] Plesniak, M. P.; Huang, H.-M.; Procter, D. J. Radical Cascade Reactions Triggered by Single Electron Transfer. *Nat. Rev. Chem.* **2017**, *1*, 1–16.

[7] Romero, K. J.; Galliher, M. S.; Pratt, D. A.; Stephenson, C. R. J. Radicals in Natural Product Synthesis. *Chem. Soc. Rev.* **2018**, *47*, 7851–7866.

[8] Narayanam, J. M. R.; Stephenson, C. R. J. Visible Light Photoredox Catalysis: Applications in Organic Synthesis. *Chem. Soc. Rev.*, **2011**, *40*, 102–113.

[9] Fu, G. C. Transition-Metal Catalysis of Nucleophilic Substitution Reactions: A Radical Alternative to S_N1 and S_N2 Processes. *ACS Cent. Sci*. **2017**, *3*, 692-700.

[10] Yan, M.; Lo, J. C.; Edwards, J. T.; Baran, P. S. Radicals: Reactive Intermediates with Translational Potential. *J. Am. Chem. Soc.* **2016**, *138*, 12692–12714.

[11] Creutz, S. E.; Lotito, K. J.; Fu, G. C.; Peters, J. C. Photoinduced Ullmann C–N Coupling: Demonstrating the Viability of a Radical Pathway. *Science* **2012**, *338*, 647–651

[12] Kainz, Q. M.; Matier, C. D.; Bartoszewicz, A.; Zultanski, S. L.; Peters, J. C.; Fu, G. C. Asymmetric Copper-Catalyzed C-N Cross-Couplings Induced by Visible Light. *Science* **2016**, *351*, 681–684.

[13] Ahn, J. M.; Ratani, T. S.; Hannoun, K. I.; Fu, G. C.; Peters, J. C. Photoinduced, Copper-Catalyzed Alkylation of Amines: A Mechanistic Study of the Cross-Coupling of Carbazole with Alkyl Bromides. *J. Am. Chem. Soc.* **2017**, *139*, 12716–12723.

[14] Chen, C.; Peters, J. C.; Fu., G. C. Photoinduced Copper-Catalysed Asymmetric Amidation via Ligand Cooperativity. *Nature*, **2021**, *596*, 250–256.

[15] Lee, H.; Ahn, J. M.; Oyala, P. H.; Citek, C.; Yin, H.; Fu, G. C.; Peters, J. C. Investigation of the C–N Bond-Forming Step in a Photoinduced, Copper-Catalyzed Enantioconvergent N–Alkylation: Characterization and Application of a Stabilized Organic Radical as a Mechanistic Probe. *J. Am. Chem. Soc.* **2022**, *144*, 4114–4123.

[16] Nakafuku, K. M.; Zhang, Z.; Wappes, E. A.; Stateman, L. M.; Chen, A. D.; Nagib, D. A. Enantioselective radical C–H amination for the synthesis of β-amino alcohols. *Nat. Chem.* **2020**, *12*, 697–704.

[17] Mao, R.; Frey, A.; Balon, J.; Hu, X. Decarboxylative C(sp^3)–N Cross-Coupling via Synergetic Photoredox and Copper Catalysis. *Nat. Catal.* **2018**, *1*, 120–126.

[18] Liang, Y.; Zhang, X.; MacMillan, D. W. C. Decarboxylative sp^3 C–N Coupling via Dual Copper and Photoredox Catalysis. *Nature* **2018**, *559*, 83–88.

[19] Demarteau, J.; Debuigne, A.; Detrembleur, C. Organocobalt Complexes as Sources of Carbon-Centered Radicals for Organic and Polymer Chemistries. *Chem. Rev.* **2019**, *119*, 6906–6955.

[20] Mondal, S.; Dumur, F.; Gigmes, D.; Sibi, M. P.; Bertrand, M. P.; Nechab, M. Enantioselective Radical Reactions Using Chiral Catalysts. *Chem. Rev.* **2022**, *122* (6), 5842–5976.

[21] Choi, J.; Fu, G. C. Transition Metal–Catalyzed Alkyl-Alkyl Bond Formation: Another Dimension in Cross-Coupling Chemistry. *Science* **2017**, *356*, eaaf7230.

[22] Sakai, H. A.; Liu, W.; Le, C. "Chip"; MacMillan, D. W. C. Cross-Electrophile Coupling of Unactivated Alkyl Chlorides. *J. Am. Chem. Soc.* **2020**, *142*, 11691–11697.

[23] Wu, X.; Hao, W.; Ye, K.-Y.; Jiang, B.; Pombar, G.; Song, Z.; Lin, S. Ti-Catalyzed Radical Alkylation of Secondary and Tertiary Alkyl Chlorides Using Michael Acceptors. *J. Am. Chem. Soc.* **2018**, *140*, 14836–14843.

[24] Claros, M.; Ungeheuer, F.; Franco, F.; Martin-Diaconescu, V.; Casitas, A.; Lloret-Fillol, J. Reductive Cyclization of Unactivated Alkyl Chlorides with Tethered Alkenes under Visible-Light Photoredox Catalysis. *Angew. Chem. Int. Ed.* **2019**, *58*, 4869–4874.

[25] Ratani, T. S.; Bachman, S.; Fu, G. C.; Peters, J. C. Photoinduced, Copper-Catalyzed Carbon–Carbon Bond Formation with Alkyl Electrophiles: Cyanation of Unactivated Secondary Alkyl Chlorides at Room Temperature. *J. Am. Chem. Soc.* **2015**, *137*, 13902–13907.

[26] Matsubara, R.; Yabuta, T.; Md Idros, U.; Hayashi, M.; Ema, F.; Kobori, Y.; Sakata, K. UVA- and Visible-Light-Mediated Generation of Carbon Radicals from Organochlorides Using Nonmetal Photocatalyst. *J. Org. Chem.* **2018**, *83*, 9381–9390.

[27] Glaser, F.; Larsen, C. B.; Kerzig, C.; Wenger, O. S. Aryl Dechlorination and Defluorination with an Organic Super-Photoreductant. *Photochem. Photobiol. Sci.* **2020,** *19*, 1035–1041.

[28] Giedyk, M.; Narobe, R.; Weiß, S.; Touraud, D.; Kunz, W.; König, B. Photocatalytic Activation of Alkyl Chlorides by Assembly-Promoted Single Electron Transfer in Microheterogeneous Solutions. *Nat Catal* **2020**, *3*, 40–47.

[29] Miller, A. J. M.; Dempsey, J. L.; Peters, J. C. Long-Lived and Efficient Emission from Mononuclear Amidophosphine Complexes of Copper. *Inorg. Chem.*, **2007**, *46*, 7244–7246.

[30] Lotito, K. J.; Peters, J. C. Efficient Luminescence from Easily Prepared Three-Coordinate Copper(I) Arylamidophosphines. *Chem. Commun.* **2010**, *46*, 3690–3692.

[31] Bergmann, L.; Friedrichs, J.; Mydlak, M.; Baumann, T.; Nieger, M.; Bräse, S. Outstanding Luminescence from Neutral Copper(I) Complexes with Pyridyl-Tetrazolate and Phosphine Ligands. *Chem. Commun.* **2013**, *49*, 6501–6503.

[32] Kim, Y.-E.; Kim, J.; Park, J. W.; Park, K.; Lee, Y. σ-Complexation as a Strategy for Designing Copper-Based Light Emitters. *Chem. Commun.* **2017**, *53*, 2858–2861.

[33] Harkins, S. B.; Peters, J. C. A Highly Emissive Cu_2N_2 Diamond Core Complex Supported by a $[PNP]^-$ Ligand. *J. Am. Chem. Soc.*, **2005**, *127*, 2030–2031.

[34] Wu, Y.; Kim, D.; Teets, T. S. Photophysical Properties and Redox Potentials of Photosensitizers for Organic Photoredox Transformations. *Synlett* **2021**, DOI: 10.1055/a-1390-9065.

[35] Kern, J.-M.; Sauvage, J.-P. Photoassisted C–C Coupling via Electron Transfer to Benzylic Halides by a Bis(Di-Imine) Copper(I) Complex. *J. Chem. Soc., Chem. Commun.* **1987**, 546–548.

[36] Cowper, N. G. W.; Chernowsky, C. P.; Williams, O. P.; Wickens, Z. K. Potent Reductants via Electron-Primed Photoredox Catalysis: Unlocking Aryl Chlorides for Radical Coupling. *J. Am. Chem. Soc.* **2020**, *142*, 2093–2099.

[37] Kim, H.; Kim, H.; Lambert, T. H.; Lin, S. Reductive Electrophotocatalysis: Merging Electricity and Light To Achieve Extreme Reduction Potentials. *J. Am. Chem. Soc.* **2020**, *142*, 2087–2092.

[38] Tian, X.; Karl, T. A.; Reiter, S.; Yakubov, S.; de Vivie-Riedle, R.; König, B.; Barham, J. P. Electro-Mediated PhotoRedox Catalysis for Selective $C(sp^3)$–O Cleavages of Phosphinated Alcohols to Carbanions. *Angew. Chem. Int. Ed.* **2021**, *60*, 20817–20825.

[39] Chernowsky, C. P.; Chmiel, A. F.; Wickens, Z. K. Electrochemical Activation of Diverse Conventional Photoredox Catalysts Induces Potent Photoreductant Activity. *Angew. Chem. Int. Ed.* **2021**, *60*, 21418–21425.

[40] Rieth, A. J.; Gonzalez, M. I.; Kudisch, B.; Nava, M.; Nocera, D. G. How Radical Are "Radical" Photocatalysts? A Closed-Shell Meisenheimer Complex Is Identified as a Super-Reducing Photoreagent. *J. Am. Chem. Soc.* **2021**, *143*, 14352–14359.

[41] Harkins, S. B.; Mankad, N. P.; Miller, A. J. M.; Szilagyi, R. K.; Peters, J. C. Probing the Electronic Structures of $[Cu_2(\mu\text{-}XR_2)]^{n+}$ Diamond Cores as a Function of the Bridging X Atom (X = N or P) and Charge (n = 0, 1, 2). *J. Am. Chem. Soc.*, **2008**, *130*, 3478–3485.

[42] Wang, Z.; Bachman, S.; Dudnik, A. S.; Fu, G. C. Nickel-Catalyzed Enantioconvergent Borylation of Racemic Secondary Benzylic Electrophiles. *Angew. Chem. Int. Ed.* **2018**, *57*, 14529–14532.

[43] Poremba, K. E.; Kadunce, N. T.; Suzuki, N.; Cherney, A. H.; Reisman, S. E. Nickel-Catalyzed Asymmetric Reductive Cross-Coupling To Access 1,1-Diarylalkanes. *J. Am. Chem. Soc.* **2017**, *139*, 5684–5687.

[44] Ju, L.; Lin, Q.; LiBretto, N. J.; Wagner, C. L.; Hu, C. T.; Miller, J. T.; Diao, T. Reactivity of (Bi-Oxazoline)Organonickel Complexes and Revision of a Catalytic Mechanism. *J. Am. Chem. Soc.* **2021**, *143*, 14458–14463.

[45] Tsentalovich, Y. P.; Fischer, H. Solvent Effect on the Decarbonylation of Acyl Radicals Studied by Laser Flash Photolysis. *J. Chem. Soc., Perkin Trans. 2* **1994**, 729–733.

[46] Marcus, R. A.; Sutin, N. Electron Transfers in Chemistry and Biology. *Biochimica et Biophysica Acta (BBA) - Reviews on Bioenergetics* **1985**, *811*, 265–322.

[47] Lovinger, G. J.; Aparece, M. D.; Morken, J. P. Pd-Catalyzed Conjunctive Cross-Coupling between Grignard-Derived Boron "Ate" Complexes and $C(sp^2)$ Halides or Triflates: NaOTf as a Grignard Activator and Halide Scavenger. *J. Am. Chem. Soc.* **2017**, *139*, 3153–3160.

[48] EPR parameters from this measurement were identical to those of isolated $[Cu_2]^+$.

[49] The remaining current is likely due to capacitive (charging) current; due to the low catalyst loading, the total current amounted to only 0.16 C.

[50] Salta, Z.; Kosmas, A. M.; Segovia, M. E.; Kieninger, M.; Tasinato, N.; Barone, V.; Ventura, O. N. Reinvestigation of the Deceptively Simple Reaction of Toluene with OH and the Fate of the Benzyl Radical: The "Hidden" Routes to Cresols and Benzaldehyde. *J. Phys. Chem. A* **2020**, *124*, 5917–5930.

[51] The reduction potential of TEMPO is −1 V vs SCE and therefore electron transfer is substantially exergonic. Reduction potential taken from: Ryan, M. C.; Whitmire, L. D.; McCann, S. D.; Stahl, S. S. Copper/TEMPO Redox Redux: Analysis of PCET Oxidation of TEMPOH by Copper(II) and the Reaction of TEMPO with Copper(I). *Inorg. Chem.* **2019**, *58*, 10194–10200.

[52] Brouillette, D.; Perron, G.; Desnoyers, J. E. Apparent Molar Volume, Heat Capacity, and Conductance of Lithium *Bis*(trifluoromethylsulfone)imide in Glymes and Other Aprotic Solvents. *J. Solution Chem.* **1998**, *27*, 151–182.